JOURNAL OF SPACECRAFT AND ROCKETS
Vol. 35, No. 4, July–August 1998

Direct Approach for Computing Near-Optimal Low-Thrust Earth-Orbit Transfers

Craig A. Kluever*
University of Missouri–Columbia, Kansas City, Missouri 64110
and
Steven R. Oleson†
NYMA, Inc., Brookpark, Ohio 44142

A new method for computing near-optimal, minimum-time Earth-orbit transfers for solar electric propulsion spacecraft has been developed. A direct optimization approach is utilized to solve the optimal control problem. The optimal thrust direction time history is computed by obtaining the optimal blend of three extremal feedback control laws. This approach is applied to long-duration orbit transfers, and the effects of Earth shadowing, oblateness, and solar cell degradation are included in the simulation. The optimal trajectories computed using the direct approach exhibit a very close match (within 1%) with the corresponding optimal trajectories obtained with a calculus of variations approach. The direct method also exhibits robust convergence properties and is insensitive to the initial guess of the optimization variables.

Nomenclature

a	= semimajor axis, km
a_T	= thrust acceleration magnitude, m/s^2
D	= solar cell degradation factor
E	= eccentric anomaly, deg
e	= eccentricity
F	= eccentric longitude, deg
G_a, G_e, G_i	= weighting functions for the respective extremal steering laws
g	= acceleration at sea level, m/s^2
h, k, p, q	= nonsingular equinoctial elements
I_{sp}	= specific impulse, s
i	= inclination, deg
J_2	= Earth oblateness coefficient
M	= 5 × 3 matrix for powered equations of motion
m	= spacecraft mass, kg
$\bar{n}$	= averaged mean motion, $\sqrt{(\mu/\bar{a}^3)}$, rad/s
P	= input power to the propulsion system, kW
R_E	= radius of the Earth, km
r	= orbital radius, km
T	= orbital period, days
t_f	= final time
$\hat{\boldsymbol{u}}_a, \hat{\boldsymbol{u}}_e$	= unit vector for the extremal in-plane steering law for maximum a', e'
v	= orbital velocity magnitude, km/s
$\boldsymbol{x}$	= state vector, $(a, h, k, p, q)^T$
$\bar{\boldsymbol{x}}$	= averaged state vector, $(\bar{a}, \bar{h}, \bar{k}, \bar{p}, \bar{q})^T$
$\hat{\boldsymbol{\alpha}}$	= 3 × 1 unit vector along the thrust direction in the equinoctial frame
γ	= orbital flight-path angle, deg
δ	= in-plane pitch steering angle, deg
η	= propulsion system efficiency
θ	= in-plane thrust steering angle, deg
μ	= Earth gravitational constant, km^3/s^2
ν	= true anomaly, deg
σ	= out-of-plane yaw steering angle, deg
Φ	= particle fluence, 1 MeV particles/cm^2
ϕ	= particle flux, 1 MeV particles/cm^2/s
Ψ	= terminal state constraints
Ω	= longitude of the ascending node, deg
ω	= argument of perigee, deg

Subscripts

en	= Earth-shadow entrance
ex	= Earth-shadow exit
f	= final
ob	= oblateness
0	= initial

Superscript

$*$	= optimal

Introduction

THE problem of obtaining optimal orbit transfers using low-thrust propulsion has been investigated in great detail. A popular topic for research involves computing minimum-fuel or minimum-time near-Earth orbit transfers for solar electric propulsion (SEP) spacecraft and examples include transfers from low Earth orbit (LEO) to geosynchronous orbit (GEO) and geosynchronous transfer orbit (GTO) to GEO. Examples of optimal near-Earth orbit transfers using low-thrust propulsion include Refs. 1–5. For SEP spacecraft with very low thrust-to-weight (T/W) ratios, the resulting orbit transfer is a slowly developing spiral trajectory with thousands of near-circular orbits about the Earth enroute to the desired final orbit. Trips times for spacecraft with T/W ratios on the order of 10^{-5} are often greater than 6 months. This characteristic significantly increases the complexity and sensitivity of the trajectory optimization problem. Furthermore, when Earth-shadow, oblateness, and solar cell degradation effects are included, the trajectory optimization problem becomes increasingly more difficult.

Low-thrust trajectory optimization techniques fall into two categories: indirect methods and direct methods. Indirect methods solve the optimal control problem by obtaining the solution to the corresponding two-point boundary value problem (2PBVP), which results from the calculus of variations. A drawback to indirect methods is that the 2PBVP is usually very sensitive and extremely difficult to solve unless a good initial guess for the unknown initial costate variables is available. An advantage of indirect methods is that if the solution to the 2PBVP is obtained, then the resulting trajectory is (in most cases) optimal. In contrast, direct methods solve

Presented as Paper 97-717 at the AAS/AIAA Astrodynamics Specialist Conference, Sun Valley, ID, Aug. 4–7, 1997; received Sept. 8, 1997; revision received Nov. 7, 1997; accepted for publication Nov. 7, 1997.

*Assistant Professor, Mechanical and Aerospace Engineering. Member AIAA.

†Senior Research Engineer, Space Propulsion Technology Section. Member AIAA.

the optimal control problem by adjusting the control variables at each iteration in an attempt to continually reduce the performance index. One advantage of direct methods is that it is usually easier to produce a good initial control guess, which typically results in a more robust optimization method. A drawback to direct methods is that convergence to the solution may be slower compared to indirect methods.

The most widely used trajectory optimization program for this class of low-thrust Earth-orbit transfers using SEP is SEPSPOT (originally SECKSPOT).[6] SEPSPOT was developed in the early 1970s and it utilizes a shooting method to solve the 2PBVP. The prospect of solving the 2PBVP is very sensitive with respect to the initial guess of the costate or adjoint variables and, therefore, this code does not possess robust convergence properties. In addition, SEPSPOT often fails to converge for cases that involve two or more of the mentioned effects (such as shadowing, oblateness, or power degradation).

This paper presents a new method for obtaining near-optimal near-Earth orbit transfers. A direct optimization approach is used to obtain the near-optimal transfer. The computation burden of numerically integrating the thousands of near-circular Earth orbits is relieved by utilizing orbital averaging techniques. The effects of Earth shadowing, oblateness, and solar cell degradation are incorporated into the orbit transfer simulation. The extremal control laws that maximize the time rates of the orbital elements are used for the thrust steering directions. We present trajectory solutions for SEP spacecraft with an initial T/W ratio of about $3(10^{-5})$. Numerical results are presented for three-dimensional LEO–GEO and GTO–GEO transfers.

Trajectory Optimization

Equations of Motion

The dynamical equations of motion for the thrusting spacecraft are presented in this section. To accommodate circular orbits ($e = 0$) and fundamental-plane orbits ($i = 0, 180$ deg), the equations of motion are written in terms of the nonsingular equinoctial elements. The relation between the equinoctial elements (a, h, k, p, q, and F) and the classical orbital elements (a, e, i, Ω, ω, and E) is given by

$$h = e\sin(\omega + \Omega) \tag{1}$$

$$k = e\cos(\omega + \Omega) \tag{2}$$

$$p = \tan(i/2)\sin\Omega \tag{3}$$

$$q = \tan(i/2)\cos\Omega \tag{4}$$

$$F = \Omega + \omega + E \tag{5}$$

The equations of motion for a spacecraft in an inverse-square gravity field and subject to a propulsive force are expressed in a compact vector-matrix form:

$$\boldsymbol{x}' = a_T M\hat{\boldsymbol{\alpha}} \tag{6}$$

In Eq. (6), the prime ($'$) indicates the derivative with respect to time. The elements of the 5×3 matrix M are presented in Ref. 3 and are shown in the Appendix. The thrust acceleration magnitude is given by

$$a_T = \frac{2\eta P_0 D(\Phi)}{mgI_{\text{sp}}} \tag{7}$$

Note that the state equation for F is not included; this is because orbital averaging is utilized and, therefore, only the slowly varying elements are considered.

The computational load of numerically simulating a long-duration, SEP orbit transfer is greatly reduced by using the method of orbital averaging.[6] Because the five orbital elements a, h, k, p, and q vary slowly with time due to the relatively small perturbing propulsion force, the average time rate of change for each respective element can be computed and large integration steps (on the order of days) can be utilized in the numerical simulation. Orbital averaging yields an approximation to Eq. (6) and is performed by calculating the incremental change in each orbital element during a single orbit and dividing by the period. The averaged time rates of change for the equinoctial elements are

$$\bar{\boldsymbol{x}}' = \frac{1}{T}\int_{F_{\text{ex}}}^{F_{\text{en}}} \bar{a}_T \bar{M}\hat{\boldsymbol{\alpha}}\,\frac{\mathrm{d}t}{\mathrm{d}F}\,\mathrm{d}F \tag{8}$$

where $\bar{\boldsymbol{x}}$ represents the approximation of the state and T is the orbital period. The overbar on the remaining variables (a_T and M) indicates evaluation using the averaged state vector $\bar{\boldsymbol{x}}$. The integral represents the incremental change in an orbital element during one revolution with all orbital elements held constant except for eccentric longitude F. The eccentric longitudes F_{ex} and F_{en} represent the exit and entrance into the Earth's shadow. The shadow exit and entrance longitudes for a given orbit and epoch date are computed by solving a quartic equation in $\cos F$ (see Ref. 6 for details). For continuous-thrust cases without Earth-shadow effects, F_{ex} and F_{en} are set to $-\pi$ and π, respectively. The term $\mathrm{d}t/\mathrm{d}F$ divided by the period T yields

$$\frac{\mathrm{d}t}{\mathrm{d}F}\frac{1}{T} = \frac{1 - \bar{k}\cos F - \bar{h}\sin F}{2\pi} \tag{9}$$

Two additional state equations are required: one equation for mass depletion and another equation for the time rate of change of the particle fluence Φ:

$$m' = \frac{2\eta P_0 D(\Phi)}{(gI_{\text{sp}})^2} \tag{10}$$

$$\Phi' = \phi \tag{11}$$

The flux ϕ is a function of orbital altitude, latitude, solar cell type, and array shield thickness (see Ref. 6 for details). Particle flux is interpolated from tabular data. The integrated particle flux (the fluence Φ) is then used to determine the solar cell damage factor $D(\Phi)$ through the use of interpolated tabular data. The damage factor is unity (no power degradation) when Φ is less than 10^{-12} particles/cm^2 and approaches zero (total power loss) as Φ approaches infinity.

The averaged state equations for mass flow rate and flux are

$$\bar{m}' = \frac{1}{T}\int_{F_{\text{ex}}}^{F_{\text{en}}} \frac{2\eta P_0 \bar{D}(\bar{\Phi})}{(gI_{\text{sp}})^2}\,\frac{\mathrm{d}t}{\mathrm{d}F}\,\mathrm{d}F \tag{12}$$

$$\bar{\Phi}' = \frac{1}{T}\int_{-\pi}^{\pi} \bar{\phi}\,\frac{\mathrm{d}t}{\mathrm{d}F}\,\mathrm{d}F \tag{13}$$

Note that the averaged flux equation (13) does not depend on the Earth-shadow conditions.

The effect of Earth oblateness (due to J_2) on the orbital transfer can be included by appending the averaged perturbation equations[5] to the respective right-hand sides of Eq. (8):

$$\bar{h}'_{\text{ob}} = \bar{\Lambda}_{hk}\bar{k} \tag{14}$$

$$\bar{k}'_{\text{ob}} = -\bar{\Lambda}_{hk}\bar{h} \tag{15}$$

$$\bar{p}'_{\text{ob}} = -\bar{\Lambda}_{pq}\bar{q} \tag{16}$$

$$\bar{q}'_{\text{ob}} = \bar{\Lambda}_{pq}\bar{p} \tag{17}$$

where

$$\bar{\Lambda}_{hk} = \frac{3\mu R_E^2 J_2[1 - 6(\bar{p}^2 + \bar{q}^2) + 3(\bar{p}^2 + \bar{q}^2)^2]}{2\bar{n}\bar{a}^5(1 - \bar{h}^2 - \bar{k}^2)^2(1 + \bar{p}^2 + \bar{q}^2)^2} \tag{18}$$

$$\bar{\Lambda}_{pq} = \frac{3\mu R_E^2 J_2(1 - \bar{p}^2 - \bar{q}^2)}{2\bar{n}\bar{a}^5(1 - \bar{h}^2 - \bar{k}^2)^2(1 + \bar{p}^2 + \bar{q}^2)} \tag{19}$$

The complete low-thrust system is governed by Eqs. (8) and (12–17).

Problem Statement

The optimal control problem treated here is a free end-time problem and involves both control functions and control parameters. In the three-dimensional setting, the problem can be stated formally as follows.

Find the optimal thrust direction time history $\hat{\boldsymbol{\alpha}}^*(t)$, $0 \leq t \leq t_f$, and the final time t_f that minimize

$$J = t_f \tag{20}$$

subject to the averaged equations of motion [Eqs. (8), (12), and (13)] with the boundary conditions at $t = 0$:

$$\bar{\boldsymbol{x}}(0) = \boldsymbol{x}_0 \tag{21}$$

$$\bar{m}(0) = m_0 \tag{22}$$

$$\bar{\Phi}(0) = \Phi_0 \tag{23}$$

and the terminal state constraints

$$\boldsymbol{\Psi}[\bar{\boldsymbol{x}}(t_f), t_f] = \bar{\boldsymbol{x}}(t_f) - \boldsymbol{x}_f = \boldsymbol{0} \tag{24}$$

The performance index (to be minimized) given in Eq. (20) is the orbit transfer time. The initial state conditions (21–23) define the initial Earth orbit, initial spacecraft mass, and initial particle fluence. The terminal state constraints (24) enforce the desired orbital elements at the end of the transfer. The goal is to compute the optimal thrust direction control $\hat{\boldsymbol{\alpha}}^*(t)$ so that the desired orbit transfer is completed in minimum time.

Solution Method

As mentioned in the Introduction, a direct approach is used to solve the trajectory optimization problem. In particular, the previously defined optimal control problem is replaced with a nonlinear programming (NLP) problem, which in turn is solved by using a gradient-based optimization method. To use a direct method, the continuous control function [the thrust steering direction $\hat{\boldsymbol{\alpha}}^*(t)$] is parameterized by a discrete number of optimization variables. Therefore, the solution to the original trajectory optimization problem is obtained by solving the associated constrained parameter optimization problem. The manner in which the control function $\hat{\boldsymbol{\alpha}}^*(t)$ is parameterized is discussed in the next section. We utilize sequential quadratic programming (SQP) to solve the constrained parameter optimization problem. The SQP code used here is NPSOL, which computes the gradients with both forward and central finite differences.[7] The terminal state constraints (24), which require matching between the final orbital elements and the desired boundary conditions, are enforced through SQP equality constraints.

Thrust Steering Laws

To minimize the end time for the orbital transfer and meet the boundary conditions of the desired final orbit, the optimal thrust direction time history $\hat{\boldsymbol{\alpha}}^*(t)$ must be computed. Because we are concerned with very low-thrust acceleration levels, the transfer time is on the order of hundreds of days, which results in thousands of orbital revolutions about the Earth enroute to the final orbit. Therefore, the prospect of parameterizing the thrust steering control function $\hat{\boldsymbol{\alpha}}(t)$ with a reasonable number of design parameters is a challenging task. A simple approach to parameterizing a continuous control function (for example, the pitch and yaw thrust steering angles) is to use linear or cubic spline interpolation through a set of discrete control parameters spaced along the time axis. However, for the problem at hand, this approach would require hundreds of design parameters (even with the use of orbital averaging) for an accurate parameterization of the control.

Our approach to parameterizing the thrust direction is to use a blend of extremal feedback control laws for the in-plane and out-of-plane steering angles. A similar approach was introduced in Ref. 3, where extremal steering laws that maximize various orbital elements were derived. The (nonoptimal) orbital transfers presented in Ref. 3 utilized separate extremal control laws for each discrete burn arc, i.e., the first burn maximized a', the second burn performed the plane change, etc. In our approach, the respective extremal steering laws are blended so that the orbital elements are controlled simultaneously and the transfer is completed in minimum time.

The first feedback control law maximizes the time rate of change of the semimajor axis a and is derived from the governing equation of motion for a:

$$a' = (2a^2 v/\mu)\, a_T \cos\theta \tag{25}$$

where θ is measured from the velocity vector to the projection of the thrust vector onto the orbit plane. The optimal in-plane steering angle that maximizes the rate a' is found by setting the partial derivative $\partial a'/\partial\theta$ equal to zero:

$$\frac{\partial a'}{\partial \theta} = -\frac{2a^2 v}{\mu} a_T \sin\theta = 0 \tag{26}$$

Therefore, the extremal steering law for maximum a' (and maximum total energy rate) is $\theta^* = 0$, i.e., align the thrust vector with the velocity vector.

The extremal feedback steering law for maximum eccentricity rate is derived in a similar fashion by observing the governing equation of motion for e:

$$e' = (a_T/v)[2(e + \cos\nu)\cos\theta + (r/a)\sin\nu\sin\theta] \tag{27}$$

Again, the partial derivative is set to zero, which yields

$$\frac{\partial e'}{\partial \theta} = \frac{a_T}{v}\left[-2(e + \cos\nu)\sin\theta + \frac{r}{a}\sin\nu\cos\theta\right] = 0 \tag{28}$$

or

$$2a(e + \cos\nu)\sin\theta = r\sin\nu\cos\theta \tag{29}$$

Therefore, the extremal steering law for e' is

$$\tan\theta^* = \frac{r\sin\nu}{2a(e + \cos\nu)} \tag{30}$$

At this point, the second partial derivative $\partial^2 e'/\partial\theta^2$ must be computed to determine if Eq. (30) maximizes or minimizes e'. Computing the partial derivative of Eq. (28) yields

$$\frac{\partial^2 e'}{\partial \theta^2} = \frac{a_T}{v}\left[-2(e + \cos\nu)\cos\theta - \frac{r}{a}\sin\nu\sin\theta\right] \tag{31}$$

The following expressions for $\sin\theta^*$ and $\cos\theta^*$ are derived from Eq. (30):

$$\sin\theta^* = \frac{r\sin\nu}{[r^2\sin^2\nu + 4a^2(e + \cos\nu)^2]^{\frac{1}{2}}} \tag{32}$$

$$\cos\theta^* = \frac{2a(e + \cos\nu)}{[r^2\sin^2\nu + 4a^2(e + \cos\nu)^2]^{\frac{1}{2}}} \tag{33}$$

Substituting Eqs. (32) and (33) into Eq. (31) yields

$$\frac{\partial^2 e'}{\partial \theta^2} = \frac{a_T}{v}\left\{\frac{-4a^2(e + \cos\nu)^2 - r^2\sin^2\nu}{a[r^2\sin^2\nu + 4a^2(e + \cos\nu)^2]^{\frac{1}{2}}}\right\} \tag{34}$$

Therefore, $\partial^2 e'/\partial\theta^2 < 0$ at every point in the orbit, which maintains that the feedback law (30) maximizes e'.

A feedback steering law for the the out-of-plane (yaw) steering angle is derived by observing the time rate equation for inclination i:

$$i' = \frac{r}{\sqrt{\mu a(1 - e^2)}}\cos(\omega + \nu) a_T \sin\sigma \tag{35}$$

where the yaw steering angle σ is measured from the orbit plane to the thrust vector. The partial derivative of Eq. (35) with respect to σ yields

$$\frac{\partial i'}{\partial \sigma} = \frac{r}{\sqrt{\mu a(1-e^2)}} \cos(\omega+\nu) a_T \cos\sigma = 0 \tag{36}$$

Therefore, a yaw steering angle of $\pm\pi/2$ results in the maximum or minimum inclination rate. The second partial derivative of Eq. (35) yields

$$\frac{\partial^2 i'}{\partial \sigma^2} = \frac{-r}{\sqrt{\mu a(1-e^2)}} \cos(\omega+\nu) a_T \sin\sigma \tag{37}$$

Because the extremal law for maximizing the inclination rate requires that $\partial^2 i'/\partial\sigma^2 < 0$, we obtain the feedback law for maximum i':

$$\sigma^* = \begin{cases} +\pi/2, & \text{if} \quad \cos(\omega+\nu) > 0 \\ -\pi/2, & \text{if} \quad \cos(\omega+\nu) < 0 \end{cases} \tag{38}$$

Although Eq. (38) provides the optimal steering law for maximizing i', any out-of-plane steering is essentially wasted when the angle $\omega+\nu$ is near ± 90 deg. Therefore, the yaw steering law

$$\sigma^* = (\pi/2)\cos(\omega+\nu) \tag{39}$$

provides a good feedback steering law for near-maximum positive inclination rate change and does not waste the thrust force near $\omega+\nu = \pm 90$ deg.

The optimal thrust steering direction $\hat{\boldsymbol{\alpha}}^*(t)$ is obtained by the optimal blend of the two in-plane feedback steering laws and the out-of-plane feedback steering law. The basic steps are as follows.

1) Compute the two unit vectors $\hat{\boldsymbol{u}}_a$ and $\hat{\boldsymbol{u}}_e$ that define the in-plane steering laws for maximum a' and e'. These unit vectors are expressed in a local radial–transverse–normal (RTN) coordinate frame where the R axis is along the radial direction, the T axis is in the orbit plane along the transverse direction, and the N axis is normal to the orbit plane. A general expression for the in-plane unit vector is

$$\hat{\boldsymbol{u}}_{a,e} = [\sin(\theta^*+\gamma), \cos(\theta^*+\gamma), 0]^T \tag{40}$$

where the flight-path angle γ is measured from the local horizon to the velocity vector. The steering angle θ^* is computed from the respective extremal feedback law.

2) Compute the blended in-plane thrust direction unit vector $\hat{\boldsymbol{u}}$ in the RTN frame

$$\hat{\boldsymbol{u}} = \frac{G_a\hat{\boldsymbol{u}}_a + G_e\hat{\boldsymbol{u}}_e}{\|G_a\hat{\boldsymbol{u}}_a + G_e\hat{\boldsymbol{u}}_e\|} = [\sin\delta, \cos\delta, 0]^T \tag{41}$$

where the values G_a and G_e are weights for each in-plane steering law and the pitch steering angle δ is measured in the orbit plane from the horizon to the projection of the thrust vector.

3) Compute the yaw steering angle by weighting Eq. (39):

$$\sigma = G_i(\pi/2)\cos(\omega+\nu) \tag{42}$$

where the weighting function G_i scales the amplitude of the yaw steering profile.

4) Compute the unit vector $\hat{\boldsymbol{\alpha}} = [\hat{\alpha}_1, \hat{\alpha}_2, \hat{\alpha}_3]^T$ along the thrust direction in the equinoctial frame from the pitch and yaw steering angles:

$$\hat{\alpha}_1 = \cos(\delta-\gamma)\cos\sigma\left(\frac{\dot{X}}{\sqrt{\dot{X}^2+\dot{Y}^2}}\right) + \sin(\delta-\gamma)\cos\sigma\left(\frac{\dot{Y}}{\sqrt{\dot{X}^2+\dot{Y}^2}}\right) \tag{43}$$

$$\hat{\alpha}_2 = -\sin(\delta-\gamma)\cos\sigma\left(\frac{\dot{X}}{\sqrt{\dot{X}^2+\dot{Y}^2}}\right) + \cos(\delta-\gamma)\cos\sigma\left(\frac{\dot{Y}}{\sqrt{\dot{X}^2+\dot{Y}^2}}\right) \tag{44}$$

$$\hat{\alpha}_3 = \sin\sigma \tag{45}$$

where $\dot{X}$ and $\dot{Y}$ are functions of the equinoctial elements and are presented in the Appendix.

The thrust direction $\hat{\boldsymbol{\alpha}}(t)$ is parameterized by the three feedback steering laws and the three weighting functions. Therefore, the optimal steering $\hat{\boldsymbol{\alpha}}^*(t)$ can be obtained by computing the optimal set of weights $G_a^*(t)$, $G_e^*(t)$, and $G_i^*(t)$ that minimize the transfer time and result in a trajectory that satisfies the boundary conditions. The weighting functions become the optimization variables in the NLP problem. Because only the relative scale of the weights is important, the weighting function $G_a(t)$ is arbitrarily set to unity for all time so that the dimension of the NLP problem is reduced. The time histories of the weighting functions $G_e^*(t)$ and $G_i^*(t)$ are obtained by linear interpolation through a discrete set of nodes. Therefore, the nodal values of the weights are the optimization variables for the NLP problem.

Numerical Results

Several optimal orbit transfers are computed for a variety of mission scenarios and simulation conditions to demonstrate the direct method. The discrete set of control nodes for G_e and G_i and the transfer time t_f are the SQP optimization variables for the NLP problem. In all cases investigated, we parameterized each weighting function with linear interpolation through 21 nodes equally spaced along the time axis. Therefore, every NLP problem consisted of 43 total optimization variables. Gaussian quadrature is used to evaluate the integrands in Eqs. (8), (10), and (11) required for orbital averaging. The averaged state equations are numerically integrated by using a standard fixed-step, fourth-order Runge–Kutta routine. A two-day integration time step was determined to be sufficient for acceptable numerical accuracy and was used in all cases.

A summary of the four mission scenarios is presented in Table 1. For all four cases, the desired final orbit is GEO with $a = 42{,}164$ km, $e = 0$, and $i = 0$ deg. Case 1 represents a spacecraft inserted into LEO by an Ariane launch vehicle. The electric propulsion thruster for case 1 is a Hall thruster. Cases 2 and 3 represent a LEO–GEO transfer with xenon ion thrusters and a Taurus launch vehicle for insertion into LEO. The initial condition for case 4 is GTO via a Taurus launch vehicle. Ion thrusters are used for the GTO–GEO transfer in case 4. All four cases involve Earth-shadow and oblateness (J_2) effects. For Earth-shadow computational purposes, the start of the orbit transfer for all cases was arbitrarily set at Jan. 1, 2000. For power

Table 1 Mission characteristics for minimum-time problems

Case	a_0 R_E	e_0	i_0, deg	Ω_0, deg	ω_0, deg	m_0, kg	I_{sp}, s	P_0, kW	η, %	Degradation effect
1	1.063	0.0	5.2	0.0	0.0	5500	1800	30	55	No
2	1.086	0.0	28.5	0.0	0.0	1200	3300	10	65	No
3	1.086	0.0	28.5	0.0	0.0	1200	3300	10	65	Yes
4	3.820	0.731	27.0	99.0	0.0	450	3300	5	65	No

degradation computational purposes, i.e., case 3, it was assumed that the solar array utilizes GaAs cells with 16 mil of shielding.

Table 2 presents a comparison of the solutions obtained by the direct method (DM) and SEPSPOT. As indicated in Table 2, the transfer times for the near-optimal solutions are less than 1% greater than the optimal transfer times computed by SEPSPOT. In addition, note that the minimum transfer time computed by the DM for the case with power degradation effects (case 3) is 8% less than the minimum transfer time obtained with SEPSPOT. This improvement in trip time can be explained by observing the transfer through the radiation belts. The trajectory computed by the DM begins the transfer by raising altitude as quickly as possible without changing the inclination whereas the trajectory computed by SEPSPOT raises altitude and decreases inclination simultaneously. Therefore, the DM trajectory completes the passage through the most severe region of the belts in a minimum-time fashion and at high latitudes where radiation dosages are attenuated. The SEPSPOT trajectory passes through the severe radiation region at a slower pace (because a plane change is also being performed) and, therefore, the solar cell degradation is worse than the DM trajectory. For example, at $t = 90$ days into the transfer, the SEPSPOT trajectory has $i = 22.7$ deg and $a = 10{,}904$ km, whereas the DM trajectory has $i = 27.5$ deg and $a = 12{,}142$ km. The accelerated passage through the radiation belts for the DM trajectory results in a final power level of 6.5 kW; the final power level of the SEPSPOT trajectory is 5.9 kW. One explanation for the inferiority of the SEPSPOT solution is that SEPSPOT has located a local minimum; this may be attributed to the initial costate guess, which was derived from a previous SEPSPOT trajectory solution that did not include degradation effects.

The time histories for semimajor axis, eccentricity, and inclination for cases 1 and 4 are presented in Figs. 1–3 and 4–6, respectively. Note that very little difference exists between the optimal (SEPSPOT) and near-optimal (DM) time histories. The pitch δ and yaw σ thrust direction angle histories for case 1 are presented in Figs. 7 and 8. Pitch and yaw histories are presented for a single revolution at the beginning, middle, and end of the orbit transfer. The steering angles are artificially set to zero when the spacecraft encounters Earth-shadow conditions. Note that the pitch steering angle follows the velocity vector during the majority of the transfer, i.e., near-tangent steering. The yaw steering angle amplitude becomes larger as the transfer progresses because inclination change is more efficient at higher altitudes and slower orbital velocities. The pitch and yaw thrust steering histories for case 4 are presented in Figs. 9 and 10. The influence of the maximum eccentricity-rate steering

Table 2 Comparison between near-optimal and optimal solutions

Case	t_f (DM), days	t_f (SEPSPOT), days	Error (SEPSPOT − DM), %
1	168.2	167.8	−0.24
2	200.3	198.8	−0.75
3	285.4	310.7	8.14
4	67.0	66.6	−0.60

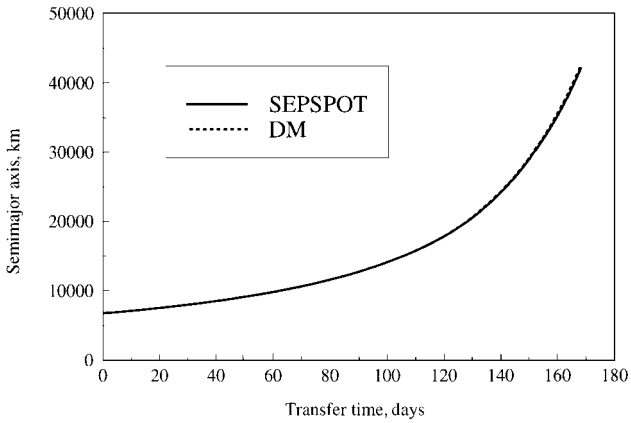

Fig. 1 Semimajor axis vs time for case 1.

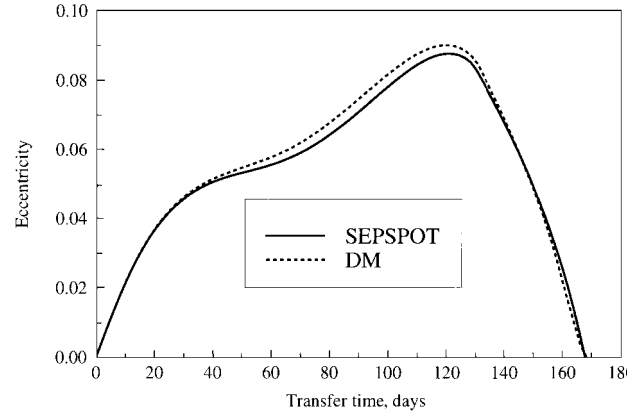

Fig. 2 Eccentricity vs time for case 1.

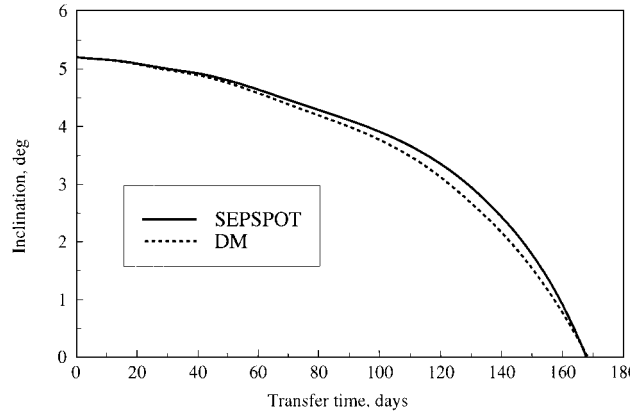

Fig. 3 Inclination vs time for case 1.

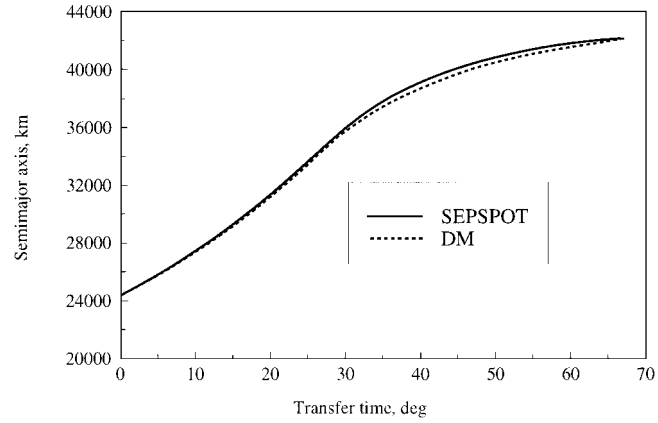

Fig. 4 Semimajor axis vs time for case 4.

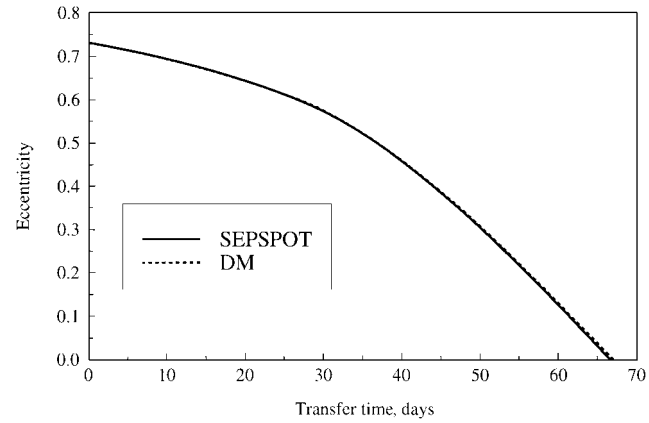

Fig. 5 Eccentricity vs time for case 4.

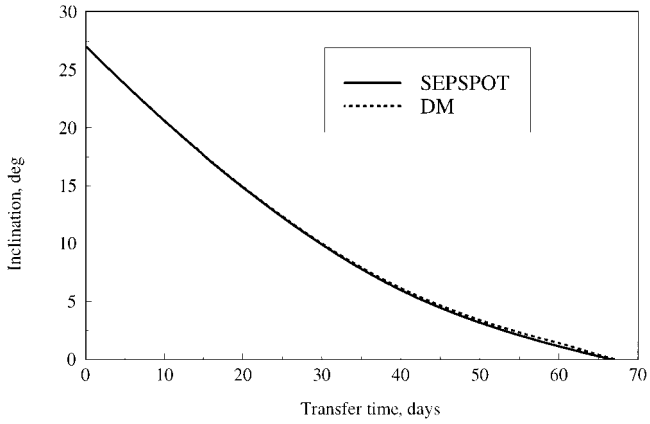

Fig. 6 Inclination vs time for case 4.

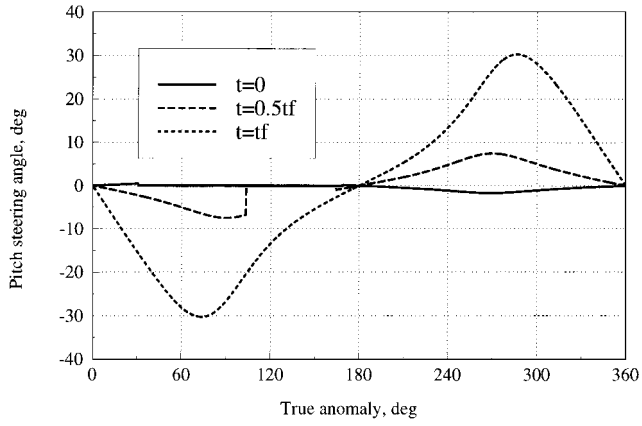

Fig. 7 Pitch steering angle vs time for case 1.

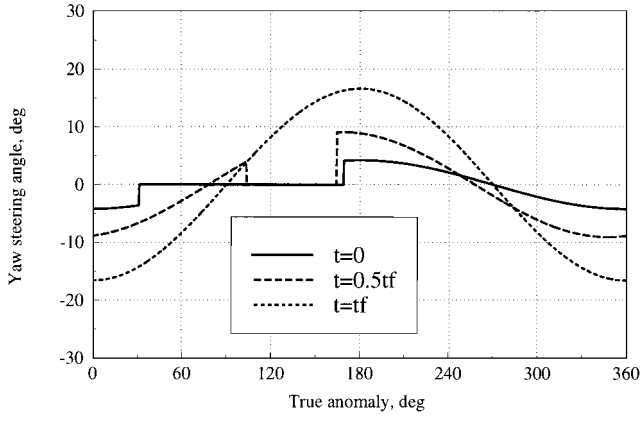

Fig. 8 Yaw steering angle vs time for case 1.

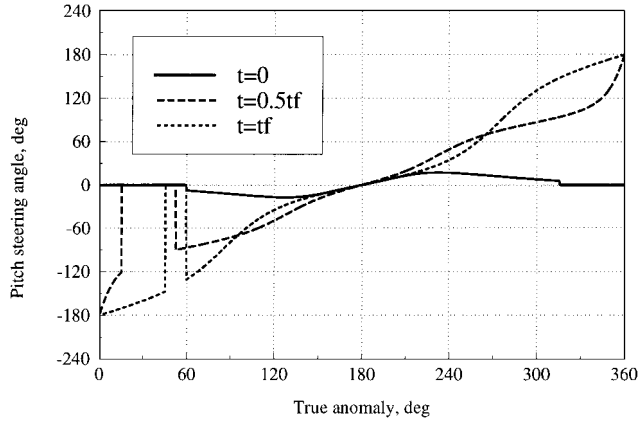

Fig. 9 Pitch steering angle vs time for case 4.

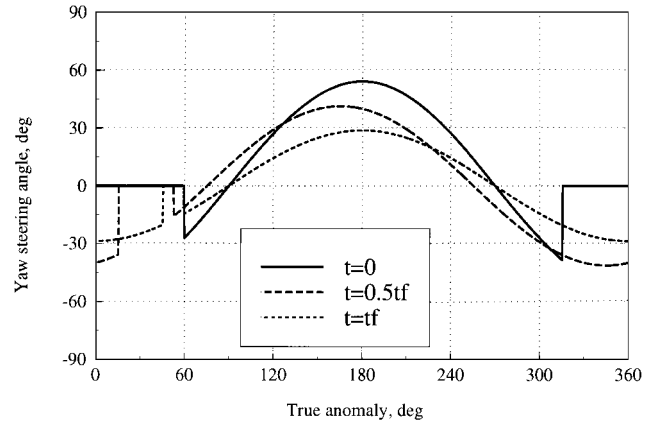

Fig. 10 Yaw steering angle vs time for case 4.

law is evident in Fig. 9 because eccentricity must be reduced from $e = 0.731$ (GTO) to zero. Note that the yaw steering is greatest at the beginning of the transfer; this occurs because the spacecraft has the slowest orbital velocity at GTO apogee as compared to the remainder of the orbit transfer and, therefore, the inclination change is most efficient at that point.

Note that a main advantage of the DM is its robust convergence property for a range of mission scenarios. All solutions presented here were obtained with an initial guess with small weights for $G_e(t)$ and $G_i(t)$, i.e., the initial guess results in a near-planar transfer with the thrust vector aligned with the velocity. The robustness of the DM is in direct contrast with SEPSPOT, which is extremely sensitive to the initial guess, i.e., the costate variables, and often experiences convergence difficulties when effects such as power degradation are included.

Conclusions

A new trajectory optimization method for computing near-optimal, minimum-time Earth-orbit transfers for SEP spacecraft has been developed. The method utilizes a direct optimization approach to solve the optimal control problem. The thrust direction time history is parameterized by combining three extremal feedback control laws and the optimal thrust steering is obtained by computing the optimal weights for each feedback law. This approach is applied to long-duration orbit transfers and the effects of Earth shadowing, oblateness, and solar cell degradation are included in the simulation. Several numerical examples are presented.

The optimal trajectories computed using the direct approach exhibit a very close match with optimal trajectories obtained with a calculus of variations approach (SEPSPOT). In a case that involves solar cell degradation effects, the DM produces an optimal trajectory with a transfer time that is less than the optimal transfer time obtained via SEPSPOT. The DM is insensitive to the initial control variable guess and displays robust convergence properties. This trajectory optimization method would be a useful preliminary design tool for mission designers.

Appendix: Matrix Elements for Equations of Motion

The elements of the matrix M from Eq. (6) are presented in this section. The additional variables introduced in the Appendix are not included in the Nomenclature inasmuch as many are dummy variables. The elements are

$$M_{11} = (2a/nr)[hkb\cos F - (1 - h^2 b)\sin F] \tag{A1}$$

$$M_{12} = (2a/nr)[(1 - k^2 b)\cos F - hkb\sin F] \tag{A2}$$

$$M_{13} = 0 \tag{A3}$$

$$M_{21} = \frac{G}{na^2}\left(\frac{\partial X}{\partial k} - hb\frac{\dot{X}}{n}\right) \tag{A4}$$

$$M_{22} = \frac{G}{na^2}\left(\frac{\partial Y}{\partial k} - hb\frac{\dot{Y}}{n}\right) \tag{A5}$$

$$M_{23} = (k/Gna^2)(qY - pX) \tag{A6}$$

$$M_{31} = -\frac{G}{na^2}\left(\frac{\partial X}{\partial h} + kb\frac{\dot{X}}{n}\right) \tag{A7}$$

$$M_{32} = -\frac{G}{na^2}\left(\frac{\partial Y}{\partial h} + kb\frac{\dot{Y}}{n}\right) \tag{A8}$$

$$M_{33} = -(h/Gna^2)(qY - pX) \tag{A9}$$

$$M_{41} = 0 \tag{A10}$$

$$M_{42} = 0 \tag{A11}$$

$$M_{43} = KY/2Gna^2 \tag{A12}$$

$$M_{51} = 0 \tag{A13}$$

$$M_{52} = 0 \tag{A14}$$

$$M_{53} = KX/2Gna^2 \tag{A15}$$

$$X = a[(1 - h^2b)\cos F + hkb\sin F - k] \tag{A16}$$

$$Y = a[(1 - k^2b)\sin F + hkb\cos F - h] \tag{A17}$$

$$\dot{X} = (a^2n/r)[hkb\cos F - (1 - h^2b)\sin F] \tag{A18}$$

$$\dot{Y} = (a^2n/r)[(1 - k^2b)\cos F - hkb\sin F] \tag{A19}$$

$$\frac{\partial X}{\partial h} = a\left[-(h\cos F - k\sin F)\left(b + \frac{h^2b^3}{1-b}\right) - \frac{a}{r}\cos F(hb - \sin F)\right] \tag{A20}$$

$$\frac{\partial X}{\partial k} = -a\left[(h\cos F - k\sin F)\frac{hkb^3}{1-b} + 1 + \frac{a}{r}\sin F(\sin F - hb)\right] \tag{A21}$$

$$\frac{\partial Y}{\partial h} = a\left[(h\cos F - k\sin F)\frac{hkb^3}{1-b} - 1 + \frac{a}{r}\cos F(kb - \cos F)\right] \tag{A22}$$

$$\frac{\partial Y}{\partial k} = a\left[(h\cos F - k\sin F)\left(b + \frac{k^2b^3}{1-b}\right) + \frac{a}{r}\sin F(\cos F - kb)\right] \tag{A23}$$

$$G = \sqrt{1 - k^2 - h^2} \tag{A24}$$

$$b = 1/(1 + G) \tag{A25}$$

$$n = \sqrt{\mu/a^3} \tag{A26}$$

$$r = a(1 - k\cos F - h\sin F) \tag{A27}$$

$$K = 1 + p^2 + q^2 \tag{A28}$$

References

[1]Redding, D. C., and Breakwell, J. V., "Optimal Low-Thrust Transfers to Synchronous Orbit," *Journal of Guidance, Control, and Dynamics*, Vol. 7, No. 2, 1984, pp. 148–155.

[2]Zondervan, K. P., Wood, L. J., and Caughey, T. K., "Optimal Low-Thrust, Three-Burn Orbit Transfers with Large Plane Changes," *Journal of the Astronautical Sciences*, Vol. 32, No. 3, 1984, pp. 407–427.

[3]Spencer, D. B., and Culp, R. D., "Designing Continuous-Thrust Low-Earth-Orbit to Geosynchronous-Earth-Orbit Transfers," *Journal of Spacecraft and Rockets*, Vol. 32, No. 6, 1995, pp. 1033–1038.

[4]Matogawa, Y., "Optimum Low Thrust Transfer to Geosynchronous Orbit," *Acta Astronautica*, Vol. 10, No. 7, 1983, pp. 467–478.

[5]Ilgen, M. R., "A Hybrid Method for Computing Optimal Low Thrust OTV Trajectories," American Astronautical Society, AAS Paper 94-129, Feb. 1994.

[6]Sackett, L. L., Malchow, H. L., and Edelbaum, T. N., "Solar Electric Geocentric Transfer with Attitude Constraints: Analysis," NASA CR-134927, Aug. 1975.

[7]Gill, P. E., Murray, W., Saunders, M. A., and Wright, M. H., "User's Guide for NPSOL (Version 4.0): a Fortran Package for Nonlinear Programming," Systems Optimization Lab., Stanford Univ., Stanford, CA, Jan. 1986.

J. A. Martin
Associate Editor